

Effects of Precipitation Temperature on Nanoparticle Surface Area and Antibacterial Behaviour of Mg(OH)₂ and MgO Nanoparticles

Banele Vatsha^{1,2}, Phumlani Tetyana¹, Poslet Morgan Shumbula¹, Jane Catherine Ngila²,
Lucky Mashudu Sikhwivhilu¹, Richard Motlhaletsi Moutloali¹

¹Advanced Materials Division, DST/Mintek Nanotechnology Innovation Centre, Mintek, Randburg, South Africa; ²Department of Applied Chemistry, University of Johannesburg, Doornfontein Campus, Johannesburg, South Africa.
Email: richardm@mintek.co.za

Received May 28th, 2013; revised June 29th, 2013; accepted July 15th, 2013

Copyright © 2013 Banele Vatsha *et al.* This is an open access article distributed under the Creative Commons Attribution License, which permits unrestricted use, distribution, and reproduction in any medium, provided the original work is properly cited.

ABSTRACT

A series of MgO nanoparticles were prepared by first precipitating and isolating Mg(OH)₂ nanoparticles from Mg(NO₃)₂ at three different temperatures using NaOH followed by their thermal decomposition also at three temperature settings. The effects of temperature at which precipitation and thermal decomposition of the hydroxide occurred were studied to assess their influence on nanoparticle size and surface area. The synthesised nanoparticles were characterized using a suite of techniques including Brunauer-Emmett-Teller (BET), X-ray diffraction (XRD), Transmission Electron Microscopy (TEM) and Scanning Electron Microscope (SEM) analysis. The average diameter range of MgO nanoparticles ranged between 15 and 35 nm, while for the precursor Mg(OH)₂ it varied between 28 and 45 nm. The nanoparticle surface area obtained from BET studies was found in all cases to increase from 77 to 106.4 m²/g with increasing temperature of precipitation. Antibacterial activities of the prepared Mg(OH)₂ and MgO nanoparticles were evaluated against the Gram-negative bacteria, *Escherichia coli*, and the Gram-positive bacteria, *Staphylococcus aureus*, using agar diffusion method. A correlation between surface area and antibacterial activity supported the mechanism of bacterial inactivation as the generation of reactive species. The Mg(OH)₂ and MgO nanoparticles both exhibited pronounced bactericidal activity towards the Gram positive bacteria than Gram negative bacteria as indicated by the extend of the zone of inhibition around the nanoparticle.

Keywords: MgO; Nanoparticles; Precipitation; Crystallinity; Antibacterial

1. Introduction

The increased proliferation of infectious diseases due to microorganisms found in medical devices, food packaging, domestic appliances and water treatment systems has elicited increased attention [1-3]. In the recent years, extensive efforts have been made to develop new or improve known materials with antimicrobial properties. Specifically, increased resistance of microorganisms towards current biocides is of great concern specifically in people of compromised immune systems like the elderly, children and the sick. This has led to increased efforts to explore new types of antimicrobial agents. In particular, inorganic oxide nanomaterials like CaO, ZnO and MgO have shown potential as effective alternatives in addressing some of these challenges [4-6]. For example, in the last decade literature exploring the use of metal ox-

ides and specifically MgO has become widespread. These studies revealed that indeed MgO is able to deactivate both gram negative and gram positive bacteria and several mechanisms of deactivation postulated [4,7]. Relationship between particle size and activity was also reported. This has led to our interest in Mg based materials for applications in health and water [8].

Current research interest in inorganic nanomaterials synthesis has focused more on controlling and tailoring materials into nanoparticles, nanorods, nanotubes, nanoplates, etc. with the aim of streamlining their applications and efficiency [6,9]. Moreover, investigations to develop versatile, cost effective and up-scalable methods in achieving predictable nanoparticle properties are paramount to the success of introducing these materials for widespread usage. These methods include sol-gel [10],

hydrothermal [11], laser vaporization, chemical gas phase deposition and combustion aerosol synthesis [12]. However, in our investigations, there are drawbacks encountered from these conventional methods that tend to give lower yield, poor control of shape and size and use of corrosive chemicals. Indeed, it is generally known that MgO's unique properties are related to the size of the nanoparticles [13]. Ouraipryvan *et al.* studied the synthesis of crystalline MgO nanoparticle with mesoporous-assembled structure via a surfactant-modified sol-gel process [14]. The obtained results showed that the particle exhibited mesoporous structure and the diameter range was approximately 35 to 50 nm. Continued search for control of nanoparticle synthesis using simple methods is still relevant.

In this study the precipitation method was adopted mainly because of its simplicity and relatively good control of the experimental conditions. The present study was carried out to investigate the effect of precipitation temperature on the morphology of MgO nanoparticles, specifically the surface area, and its influence on antibacterial (*E. coli* and *S. aureus*) activity. A strong correlation between nanoparticle surface area and antibacterial effects was observed giving an indirect way of establishing mechanism of bacterial inactivation.

2. Experimental Section

2.1. Materials

Magnesium nitrate (Mg(NO₃)₂), sodium hydroxide (NaOH) were purchased from Sigma Aldrich, South Africa. All solutions were prepared using freshly prepared high purity water from a Millipore unit, Q-POD. *Escherichia coli* (*E. coli*) and *Staphylococcus aureus* (*S. aureus*) strain were donated by Biolabels Unit at Mintek.

2.2. Characterisation Techniques

The XRD diffractograms were recorded on a Bruker D8 Advance X-ray diffractometer using a Co-K α (1.7902Å) monochromatic radiation source and a Ni filter with the operating voltage and current maintained at 40 kV and 40 mA respectively in the 2 θ range of 5° - 80°. The obtained diffraction patterns were processed using Eva software. Differential scanning calorimetric (DSC) analysis were performed using air as oxidant at the heating rate of 10°C·min⁻¹ in a crimped aluminium crucible heated up to a temperature of 500°C using a Shimadzu DSC60 instrument with a TA60WS thermal analyser and FC60A controller. Scanning electron microscopy (SEM) analyses were done on a Nova NanoSEM 200 from FEI operating at 10.0 KV. The Transmission Electron Microscopy (TEM) images were acquired on a Philips CM120 Biotwin Transmission Electron Microscope. The samples

were prepared by placing a drop of a dilute sample on a carbon-coated copper grid (400 mesh, agar). The samples were allowed to dry completely at room temperature. Nitrogen adsorption measurements were performed at 77 K using a Micromeritics ASAP2010 system utilizing Brunauer Emmett-Teller (BET) calculations for surface area and BJH calculations for pore size distribution for the desorption branch of the isotherm.

2.3. Synthesis and Characterisation of Magnesium Oxide Nanoparticles

Mg(NO₃)₂ (0.2 M) and NaOH (0.4 M) solutions were prepared using deionized water from Millipore water purification system. Precipitation was induced by dropwise addition of NaOH into the Mg(NO₃)₂ solution under continuous stirring for 1 hour at different reaction temperatures (*i.e.* 23°C, 60°C and 85°C) at pH 12. The reaction mixture was cooled down to room temperature, centrifuged and washed with copious amount of high purity water and ethanol for effective removal of impurities. The final product was dried at 80°C for 24 h and calcined at different temperatures (*i.e.* 500°C, 600°C and 700°C). **Table 1** summarises the materials used and reaction conditions.

2.4. Antibacterial Study Using Agar Diffusion Method

Antibacterial activity was performed using agar diffusion method adopted from Sundrarajan *et al.*, [13]. Bacterial cultures were grown overnight at 37°C by adding a single colony in 100 ml Luria Bertani Broth. *E. coli* and *S. aureus* cultures (0.1 ml each) were plated out onto individual Nutrient Agar plates using the Aseptic technique. Holes/Wells were made on the nutrient agar inoculated with bacteria and (about 0.5 mg) MgO nanoparticle suspensions were decanted into the wells and the plates

Table 1. Precipitation and calcination temperatures used for MgO nanoparticle synthesis.

Type	Sample	Precipitation temperature (°C)	Calcination temperature (°C)
A	1	23	500
	2	23	600
	3	23	700
	4	60	500
B	5	60	600
	6	60	700
	7	85	500
C	8	85	600
	9	85	700

incubated overnight at 37°C. Finally, the diameters of zones of inhibition around the wells were measured against the control strain and measured with callipers. Zone of inhibition is the area in which the bacterial growth is stopped due to bacteriostatic effect of the compound and it measures the inhibitory effect of compound towards a particular microorganism.

3. Results and Discussion

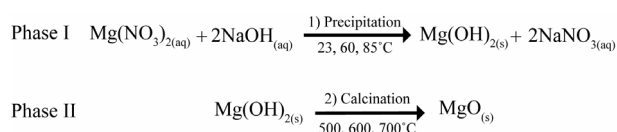
3.1. Preparation of MgO from Mg(OH)₂ Nanoparticles

The synthesis protocol employed for MgO nanoparticles was a precipitation-calcination method. This involved dropwise addition of sodium hydroxide into aqueous solution of magnesium nitrate at various temperatures between 25°C to 85°C to induce precipitation to form of magnesium hydroxide. In order to finally obtain MgO nanoparticles, the Mg(OH)₂ powder was calcined at 500°C, 600°C and 700°C through the decomposition of Mg(OH)₂ to MgO nanoparticles (Scheme 1).

Temperature of precipitation is one method of manipulating nanoparticle size and morphology. For example, Yildirim and Duncan observed that the size of spherical ZnO nanoparticles could be manipulated by the choice of precipitation temperature (13.0 ± 1.9 nm at 25°C and 9.0 ± 1.3 nm at 80°C), which they attributed to changes in the nature of adsorption events between ZnO crystals and organic molecules used as surfactants [15]. Even though, no surfactants were used in the current method, good control and manipulation of nanoparticle morphologies were obtained by varying the precipitation temperature. This indicates that precipitation temperature might be an important factor in controlling morphologies in instances of ionic effects rather surfactants are being used. This will assist in lowering the overall cost associated with controlled nanoparticle synthesis. It is however important to note that many methods and their variants have been used to produce MgO nanoparticles [16-24].

3.2. Thermal Analysis of the Mg(OH)₂ Transformation to MgO

Figure 1 shows the DSC and TGA profiles of the decomposition and transformation of Mg(OH)₂ nanoparticles into MgO nanoparticles. The thermograms are do-



Scheme 1. MgO derived from Mg(NO₃)₂ precursor reaction mechanism through the Mg(OH)₂ intermediate.

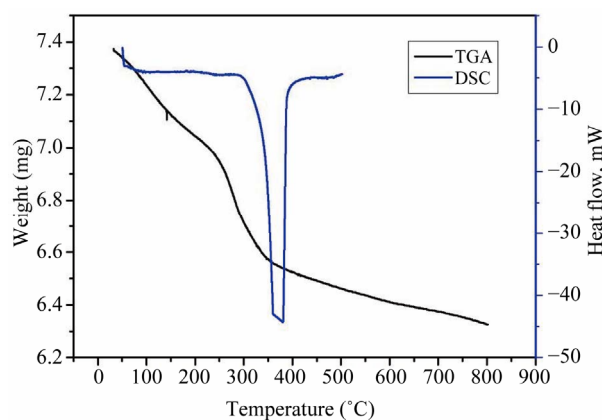


Figure 1. TGA and DSC profiles of the decomposition of the prepared Mg(OH)₂ to MgO nanoparticles.

minated by one major thermal event centred on 380°C (DSC) with an onset at 250°C (TGA) or 280°C (DSC). This onset marks the start of the decomposition of Mg(OH)₂ to MgO nanoparticles which occurs typically during calcination of the hydroxide material [11,18, 25-27]. Other thermal events observed were in the temperature regions around 100°C, 240°C and 465°C. The first event at 100°C is probably related to the loss of physically adsorbed or unbound water molecules on the hydroxide. The thermal event around 240°C is generally attributed to the loss of chemisorbed water molecules [28]. The thermal event at 465°C that occurs after the transformation of the hydroxide to the oxide is associated with the phase transformation of amorphous MgO into its cubic ordered phase [27]. This event, however, is not widely reported or observed in literature during thermal transformation of Mg(OH)₂ to MgO.

3.3. X-Ray Characterisation of Mg(OH)₂ and MgO Nanoparticles

Figure 2 depicts the X-ray diffractogram of Mg(OH)₂ nanoparticles precipitated at different temperatures, viz. A at 23°C, B at 60°C and C at 85°C. The three diffractograms are similar and exhibit the same diffraction pattern associated with Mg(OH)₂ materials. The multiple diffraction peaks from Mg(OH)₂ at 22°, 44°, 60°, 69°, 74°, 82° and 86° arise from the 001, 100, 011, 012, 110, 200 and 021 planes respectively according to a report by Sundrarajan *et al.* [13] and the XRD PDF2010: 000021169. This confirmed that the formation of pure Mg(OH)₂ nanoparticles is indifferent to the precipitation temperature used.

Figure 3 is the X-ray diffractograms of MgO nanoparticles produced by calcining Mg(OH)₂ at different temperatures. The nanoparticles produced by calcination at 500°C (A), 600°C (B) and 700°C (C) all exhibited identical diffraction patterns. The samples all had diffraction

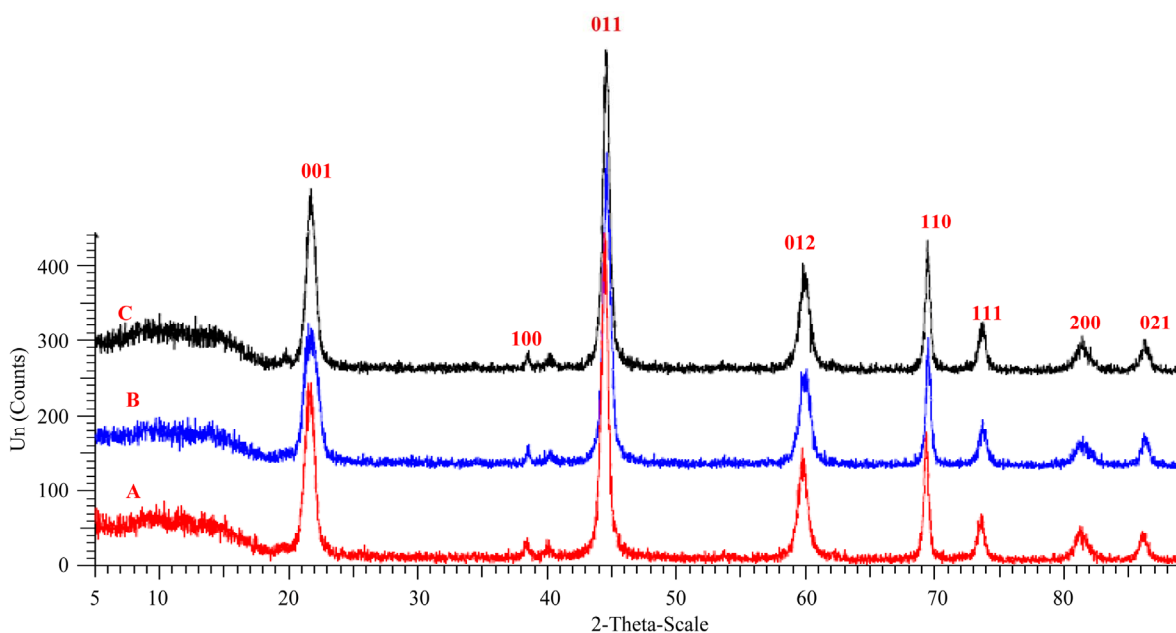


Figure 2. Comparison of X-ray diffractograms of Mg(OH)₂ nanoparticles precipitated at 23°C (A), 60°C (B) and 85°C (C).

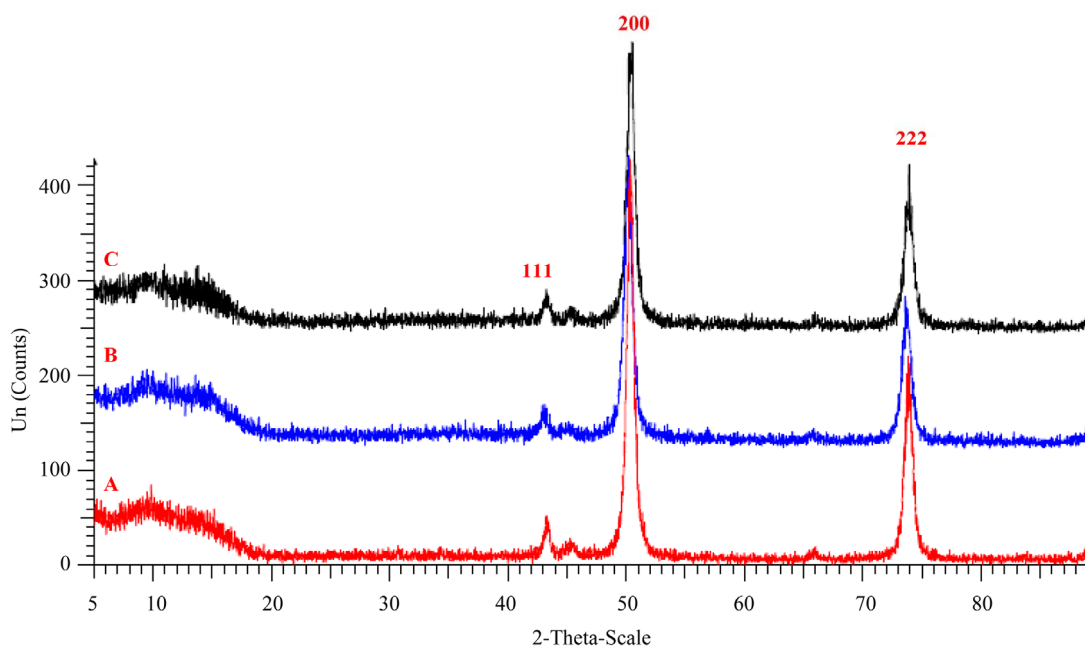


Figure 3. X-ray diffractograms of MgO particles prepared from Mg(OH)₂ precipitated at 23°C (A), 60°C (B) and 85°C (C).

peaks at 44°, 50° and 74° are assigned to 111, 200 and 222 planes respectively (XRD PDF2010:000021207). This clearly indicated that Mg(OH)₂ was completely transformed to crystalline MgO with no traces of impurities observed. The results also show that calcining at the relatively low temperature of 500°C is adequate to produce pure MgO using this method. The crystallite sizes (Table 2) were also calculated on the samples using 111, 200 and 220 diffraction maxima from the half-width of

diffraction peaks using Scherrer's equation. The calculated crystallite sizes are comparable (on the lower end) with the sizes obtained from TEM analysis for MgO nanoparticles. According to the XRD data, the mean crystallite sizes of the MgO nanoparticles were calculated by using the Debye Scherrer formula.

$$D = \frac{0.9\lambda}{\beta \cos \theta}$$

Table 2. BET results of MgO nanoparticles calcined at 700°C.

Sample name (precipitation temperature)	Surface area (m ² /g)	XRD crystallite sizes (nm)		
		(111)	(200)	(220)
Mg(OH) ₂ (23°C)	77.6	18.5	18.8	17.5
Mg(OH) ₂ (60°C)	88.1	10.7	15.3	15.3
Mg(OH) ₂ (85°C)	106.4	13.7	16.3	15.0

where λ = cobalt wavelength (1.7902Å), θ is the bragg diffraction angle of the XRD peak, β is the measured broadening of the diffraction line peak at an angle 2θ , at half its maximum intensity (FWHM) in radian.

3.4. BET Analysis of Mg(OH)₂ and MgO Nanoparticles

The BET method was used to obtain specific surface area for the MgO nanoparticles. BJH analysis was used to determine the pore size distribution. This indicated that MgO nanoparticles exhibit a bimodal pore distribution which contains mesopores of between 1.7 - 5.2 nm and larger mesopores with pore size averaging at 34.0 nm. Rezaei *et al.* observed that the specific surface area of the nanoparticles increased with increasing refluxing time and temperature [29]. This is in line with our results that showed that nanoparticles produced at different precipitation temperature showed that the specific surface area increased with an increase in precipitation temperature (**Table 2**).

3.5. TEM Analysis of Mg(OH)₂ and MgO Nanoparticles

TEM was used to analyse Mg(OH)₂ nanoparticles precipitated at different temperatures. The general observation was that the shapes appear to be different (**Figure 4**). It would be interesting to interrogate this observation further but due to no access to a TEM instrument with higher resolution, this idea was not explored further. The average size distribution of the nanoparticles is shown in **Figure 4** with a mean of 37 nm for Mg(OH)₂ precipitated at 25°C (**Figure 4(a)**), 28 nm for those produced at 60°C (**Figure 4(b)**) and 45 nm for those precipitated at 85°C (**Figure 4(c)**). Literature shows that precipitation temperature has an influence on the shapes and not size, with flakes being observed when lower temperatures are used [13,30,31]. Others have recently reported that there is a correlation between precipitation temperature and final particle size as long as the reaction is allowed to progress for longer periods at lower temperatures to allow complete reaction and other processes to take place [32]. This aspect however widely reported, gives conflicting conclusions in literature to result in one predictive approach.

In the current work indications are that the size variance does not show an obvious relationship with the precipitation temperature used an observation that was also made by Lv *et al.* [33].

MgO nanoparticles prepared by calcination of Mg(OH)₂ materials at different temperatures, *viz.* 500, 600 and 700°C were also characterised using TEM. The overall average size range determined by TEM analysis results ranged from 14 to 32 nm (**Table 3**). The average size of nanoparticles obtained at 500 and 600°C were comparable irrespective of the precipitation temperature used to produce Mg(OH)₂ particles with a narrow distribution between 14 and 20 nm. On the other hand, nanoparticles obtained at 700°C were relatively larger (between 27 and 32 nm). Even though the general observation was that all calcination temperatures resulted in average sizes of less than 35 nm, the general appearance of the nanoparticles seemed different. Sundrarajan *et al.* also observed the effects temperature had on the morphology of MgO nanoparticles where the initial flakes were transformed as the calcination temperature was increased [13]. In so far as the precipitation temperature was concerned, it was observed that nanoparticles precipitated at higher temperature (85°C) exhibited more defined shapes compared to those obtained at 23°C and 60°C, indicating that nanoparticle shape and size might be influenced by the precipitation temperature of the precursor Mg(OH)₂ powder was produced. Mageshwari and Sathyamoorthy used a precipitation temperature of 100°C to produce MgO nanoparticles with a 5 nm average, an observation that indicates that other parameters are more important at controlling particle size than precipitation temperature [34].

3.6. Antibacterial Studies

The antibacterial effects of Mg(OH)₂ and MgO nanoparticles were investigated using gram negative and gram positive bacterial strains, *E. coli* and *S. aureus* respectively, by the well diffusion agar method. The zones of inhibition, the clearing zones around the wells without visible bacterial growth, were measured from three separate plates and are captured in **Figure 5**. These zones indicate the antibacterial activity of Mg(OH)₂ and MgO since no bacterial growth is observed in those areas. The antibacterial activity, from both Mg(OH)₂ and MgO, was higher in *S. aureus* than that observed in *E. coli* tests. This can be attributed in part to the general observation that gram positive bacterial strains are more susceptible to antibacterial materials as compared to gram negative strains due to differences in their cell wall structure [35]. On the other hand, MgO exhibited consistently higher activity against *S. aureus* bacteria than Mg(OH)₂ (**Figure 5**). This is in line with literature observation by Panacek *et al.* [36] and Pan *et al.* [37] that smaller nanoparticles

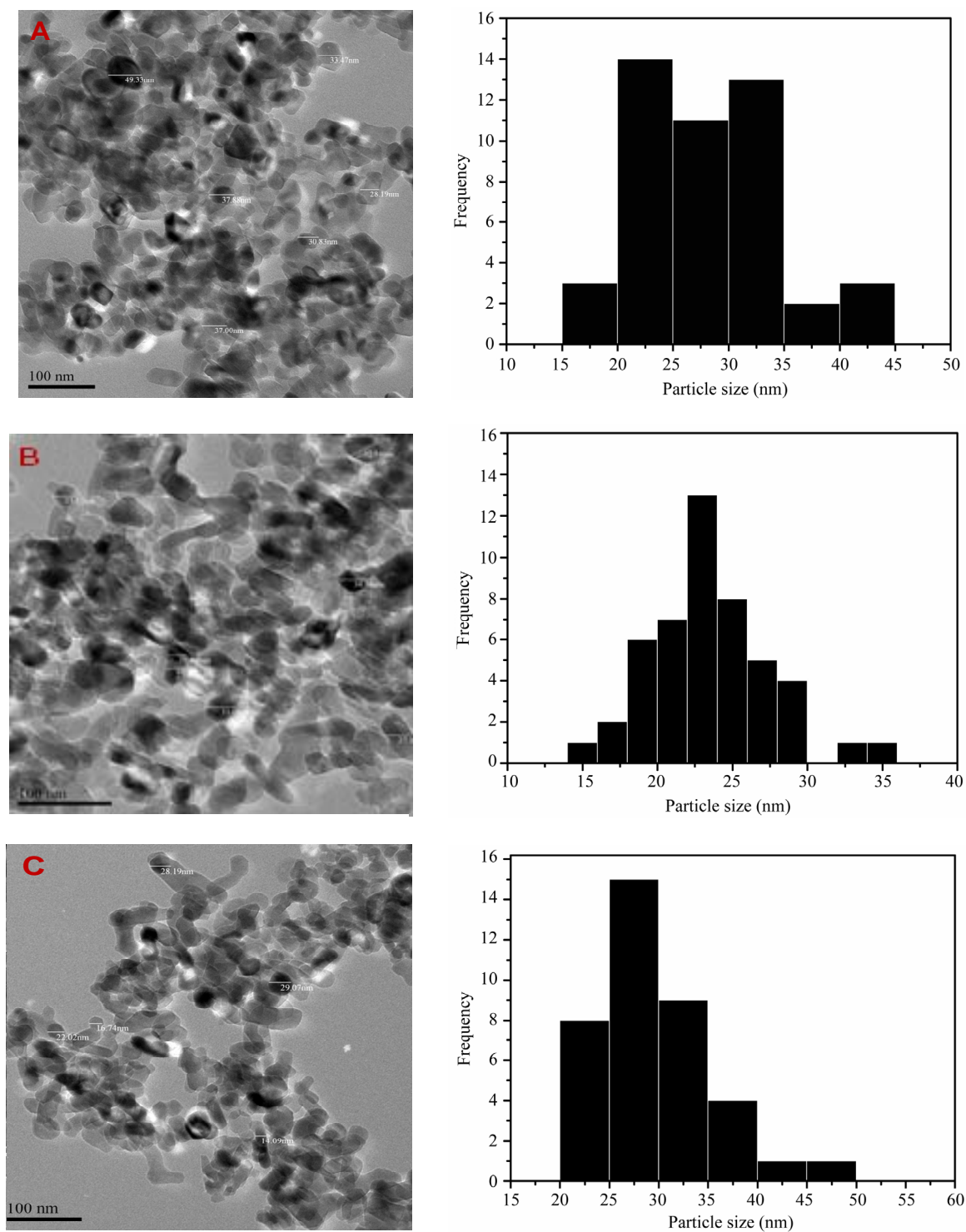


Figure 4. TEM micrographs of MgO nanoparticles calcined at 700°C (C) from $\text{Mg}(\text{OH})_2$ precipitated 23°C (A), 60°C (B), 85°C (C) and with their respective histograms generated from the TEM micrographs.

are more active than larger ones and thus MgO nanoparticles, which are smaller than $\text{Mg}(\text{OH})_2$ nanoparticles, are more effective towards inhibition of bacterial growth. The mechanism of bacterial inhibition for nanoparticle is

usually attributed to the generation of reactive radicals [38]. This mechanism is also assumed in this study and therefore the different antibacterial activities of the materials are related to their ability to generate such radicals,

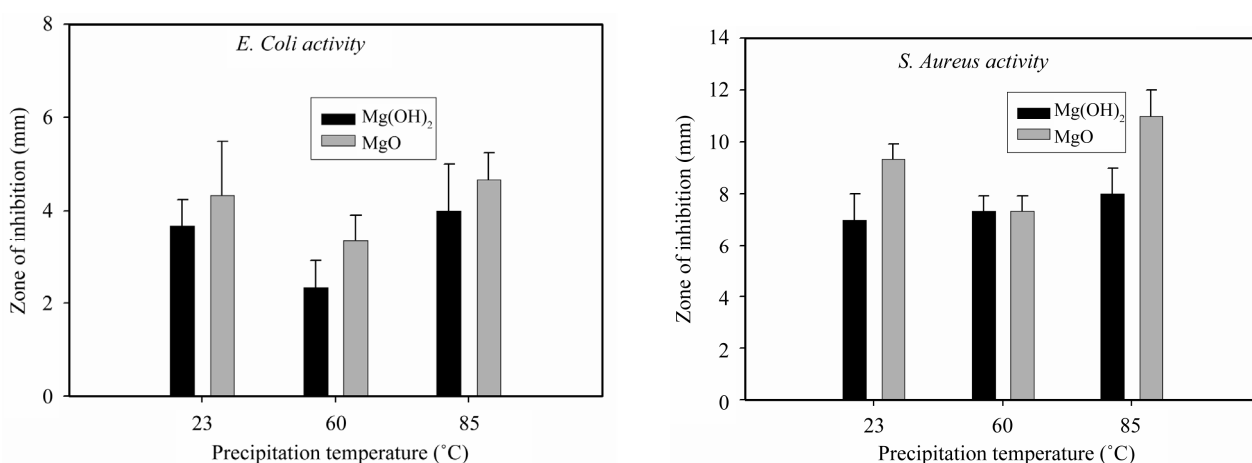


Figure 5. Antibacterial activities of Mg(OH)₂ and MgO as measured by zone of inhibition method.

Table 3. Summary of preparation conditions and average nanoparticle sizes (nm).

Precipitation temperature (°C)	Calcination temperature (°C)	500	600	700	Mg(OH) ₂
25		15	14	27	37
60		16	18	23	28
85		18	20	32	45

Table 4. Relationship of MgO (calcined at 700°C) antibacterial activity towards *S. aureus* and surface area.

Precipitation temperature	Activity against <i>S. aureus</i> (mm)		Surface area MgO	MgO (nm) 700°C	Mg(OH) ₂ (nm)
	Mg(OH) ₂	MgO			
23	6.5	8.6	77.6	27	37
60	6.8	7.0	88.1	23	28
85	7.5	10.2	104.2	32	45

a property that is dependent on the surface area and crystal edges exposed. It is known that the higher the surface area per unit mass, the more reactive material becomes. The density of radicals produced, and hence the inhibition ability is directly related to this property and hence the trends observed in this study (Table 4). For example, MgO is known to be more reactive than its hydroxide and hence the activity trend observed whereby the oxide is more active than the analogous hydroxide in all cases studied. Within the materials themselves, e.g. oxides, the activity trend follows the surface area and nanoparticle size trend established in prior sections.

4. Conclusion

Synthesis and antibacterial effects of Mg(OH)₂ and MgO nanoparticles were undertaken and factors contributing to the formation of well-defined nanoparticles were explored. Temperature at which calcination of Mg(OH)₂ to MgO was performed was found to be more important than the temperature at which Mg(OH)₂ was synthesised in determining the final MgO nanoparticle size. A simple and cost effective method to obtain nanoparticles with narrow size dispersion was established in this study. The antibacterial activities of the prepared Mg(OH)₂ and MgO nanoparticles were studied using well-diffusion method. Both these nanoparticle types exhibited greater

antibacterial effects towards Gram-positive bacteria than Gram-negative ones. In all cases, the antibacterial activity of Mg(OH)₂ was lower than that of MgO, i.e. against both *E. coli* and *S. aureus*. The antibacterial activity was closely related to the surface area than to the actual nanoparticle size observed. The relatively low cost and abundance of Mg based nanoparticles (Mg(OH)₂ and MgO) versus other metal based antibacterial agents make this material a viable alternative for this application, i.e. *E. coli* and *S. aureus* inhibition.

REFERENCES

- [1] D. Lee, R. E. Cohen and M. F. Rubner, "Antibacterial Properties of Ag Nanoparticle Loaded Multilayers and Formation of Magnetically Directed Antibacterial Microparticles," *Langmuir*, Vol. 21, No. 21, 2005, pp. 9651-9659. <http://dx.doi.org/10.1021/la0513306>
- [2] L.-A. B. Rawlinson, S. A. M. Ryan, G. Mantovani, J. A. Syrett, D. M. Haddleton and D. J. Brayden, "Antibacterial Effects of Poly(2-(Dimethylamino Ethyl)Methacrylate) against Selected Gram-Positive and Gram-Negative Bacteria," *Biomacromolecules*, Vol. 11, No. 2, 2009, pp. 443-453. <http://dx.doi.org/10.1021/bm901166y>
- [3] M. Fernandez-Garcia and A. Munoz-Bonilla, "Polymeric Materials with Antimicrobial Activity," *Progress in Polymer Science*, Vol. 37, No. 2, 2012, pp. 281-339.

- <http://dx.doi.org/10.1016/j.progpolymsci.2011.08.005>
- [4] P. K. Stoimenov, R. L. Klinger, G. L. Marchin and K. J. Klabunde, "Metal Oxide Nanoparticles as Bactericidal Agents," *Langmuir*, Vol. 18, No. 17, 2002, pp. 6679-6686. <http://dx.doi.org/10.1021/la0202374>
- [5] A. G. Nasibulin, L. Sun, S. HaaMaaLainen, S. D. Shandakov, F. Banhart and E. I. Kauppinen, "In Situ TEM Observation of MgO Nanorod Growth," *Crystal Growth & Design*, Vol. 10, No. 1, 2009, pp. 414-417. <http://dx.doi.org/10.1021/cg9010168>
- [6] Y. G. Zhang, H. Y. He and B. C. Pan, "Structural Features and Electronic Properties of MgO Nanosheets and Nanobelts," *The Journal of Physical Chemistry C*, Vol. 116, No. 43, 2012, pp. 23130-23135. <http://dx.doi.org/10.1021/jp3077062>
- [7] K. Krishnamoorthy, J. Y. Moon, H. B. Hyun, S. K. Cho and S. J. Kim, "Mechanistic Investigation on the Toxicity of MgO Nanoparticles toward Cancer Cells," *Journal of Materials Chemistry*, Vol. 22, No. 47, 2012, pp. 24610-24617. <http://dx.doi.org/10.1039/c2jm35087d>
- [8] L. Bertinetti, C. Drouet, C. Combes, C. Rey, A. Tampieri, S. Coluccia and G. Martra, "Surface Characteristics of Nanocrystalline Apatites: Effect of Mg Surface Enrichment on Morphology, Surface Hydration Species, and Cationic Environments," *Langmuir*, Vol. 25, No. 10, 2009, pp. 5647-5654. <http://dx.doi.org/10.1021/la804230j>
- [9] A. Sternig, S. Klacar, J. Bernardi, M. StoGer-Pollach, H. GroNbeck and O. Diwald, "Phase Separation at the Nanoscale: Structural Properties of BaO Segregates on MgO-Based Nanoparticles," *The Journal of Physical Chemistry C*, Vol. 115, No. 32, 2011, pp. 15853-15861. <http://dx.doi.org/10.1021/jp204043g>
- [10] V. M. Boddu, S. Dabir, Y. Viswanath and S. W. Maloney, "Synthesis and Characterization of Coralline Magnesium Oxide Nanoparticles," *Journal of American Ceramic Society*, Vol. 91, No. 5, 2008, pp. 1718-1720. <http://dx.doi.org/10.1111/j.1551-2916.2008.02344.x>
- [11] G. Wang, L. Zhang, H. Dai, J. Deng, C. Liu, H. He and C. T. Au, "Assisted Hydrothermal Synthesis and Characterization of Rectangular Parallelepiped and Hexagonal Prism Single-Crystalline MgO with Three-Dimensional Wormhole Like Mesopores," *Inorganic Chemistry*, Vol. 47, No. 10, 2008, pp. 4015-4022. <http://dx.doi.org/10.1021/ic7015462>
- [12] J. C. Yu, A. Xu, L. Zhang, R. Song and L. Wu, "Synthesis and Characterization of Porous Magnesium Hydroxide and Oxide Nanoplates," *Journal of Physical Chemistry B*, Vol. 108, No. 1, 2004, pp. 64-70. <http://dx.doi.org/10.1021/jp035340w>
- [13] S. Sundarajan and S. Ramakrishna, "Fabrication of Nanocomposite Membranes from Nanofibers and Nanoparticles for Protection against Chemical Warfare Stimulants," *Journal of Materials Science*, Vol. 42, No. 20, 2007, pp. 8400-8407. <http://dx.doi.org/10.1007/s10853-007-1786-4>
- [14] P. Ouraipryvan, T. Sreethawong and S. Chavadej, "Synthesis of Crystalline MgO Nanoparticle with Mesoporous-Assembled Structure via a Surfactant-Modified Sol-Gel Process," *Materials Letters*, Vol. 63, No. 21, 2009, pp. 1862-1865.
- [15] O. A. Yıldırım and C. Duncan, "Effect of Precipitation Temperature and Organic Additives on Size and Morphology of ZnO Nanoparticles," *Journal of Materials Research*, Vol. 27, No. 11, 2012, pp. 1452-1461. <http://dx.doi.org/10.1557/jmr.2012.58>
- [16] H. C. Bajaj, I. Mukhopadhyay and A. B. Panda, "Controlled Synthesis of Different Morphologies of MgO and Their Use as Solid Base Catalysts," *Journal of Physical Chemistry C*, Vol. 115, No. 25, 2011, pp. 12308-12316. <http://dx.doi.org/10.1021/jp2022314>
- [17] N. Budiredla, A. Kumar, S. Thota and J. Kumar, "Synthesis and Optical Characterization of Mg_{1-x}Ni_xO Nanostructures," *ISRN Network Nanomaterials*, Vol. 2012, 2012, Article ID: 865373.
- [18] X. L. Cao, C. Cheng, Y. L. Ma and C. S. Zhao, "Preparation of Silver Nanoparticles with Antimicrobial Activities and the Researches of Their Biocompatibilities," *Journal of Materials Science*, Vol. 21, No. 10, 2010, pp. 2861-2868.
- [19] P. P. Fedorov, E. A. Tkachenko, S. V. Kuznetsov, V. V. Voronov and S. V. Lavrishchev, "Preparation of MgO Nanoparticles," *Inorganic Materials*, Vol. 43, No. 5, 2007, pp. 502-504. <http://dx.doi.org/10.1134/S0020168507050111>
- [20] M. Haertelt, A. Fielicke, G. Meijer, K. Kwapien, M. Sierka and J. Sauer, "Structure Determination of Neutral MgO Clusters-Hexagonal Nanotubes and Cages," *Physical Chemistry Chemical Physics*, Vol. 14, No. 8, 2012, pp. 2849-2856. <http://dx.doi.org/10.1039/c2cp23432g>
- [21] J. Hu, Z. Song, L. Chen, H. Yang, J. Li and R. Richards, "Adsorption Properties of MgO (111) Nanoplates for the Dye Pollutants from Wastewater," *Journal of Chemical Engineering Data*, Vol. 55, No. 9, 2010, pp. 3742-3748. <http://dx.doi.org/10.1021/jc100274e>
- [22] F. Khairallah and A. Glisenti, "Synthesis, Characterization and Reactivity Study of Nanoscale Magnesium Oxide," *Journal of Molecular Catalysis A: Chemical*, Vol. 274, No. 1-2, 2007, pp. 137-147. <http://dx.doi.org/10.1016/j.molcata.2007.04.039>
- [23] A. O. Menezes, P. S. Silva, E. P. Hernandez, L. E. P. Borges and M. A. Fraga, "Tuning Surface Basic Properties of Nanocrystalline MgO by Controlling the Preparation Conditions," *Langmuir*, Vol. 26, No. 5, 2010, pp. 3382-3387. <http://dx.doi.org/10.1021/la903149v>
- [24] H. Niu, Q. Yang, K. Tang and Y. Xie, "Large-Scale Synthesis of Single-Crystalline MgO with Bone-Like Nanostructures," *Journal of Nanoparticle Research*, Vol. 8, No. 6, 2006, pp. 881-888.
- [25] F. Meshkani and M. Rezaei, "Facile Synthesis of Nanocrystalline Magnesium Oxide with High Surface Area," *Powder Technology*, Vol. 196, No. 1, 2009, pp. 85-88. <http://dx.doi.org/10.1016/j.powtec.2009.07.010>
- [26] F. Meshkani and M. Rezaei, "Effect of Process Parameters on the Synthesis of Nanocrystalline Magnesium Oxide with High Surface Area and Plate-Like Shape by Surfactant Assisted Precipitation Method," *Powder Technology*, Vol. 199, No. 2, 2010, pp. 144-148.

- <http://dx.doi.org/10.1016/j.powtec.2009.12.014>
- [27] L.-Z. Pei, L. Z. Yin, J. F. Wang, J. Chen, C. G. Fan and Q. F. Zhang, "Low Temperature Synthesis of Magnesium Oxide and Spinel Powders by a Sol-Gel Process," *Journal of Materials Research*, Vol. 13, No. 3, 2010, pp. 339-343. <http://dx.doi.org/10.1590/S1516-14392010000300010>
- [28] M. F. Parveen, S. Umapathy, V. Dhanalakshmi and R. Anbarasan, "Synthesis and Characterization of Nanosized Mg(OH)₂ and Its Nanocomposite with Poly(Vinyl Alcohol)," *NANO: Brief Reports and Reviews*, Vol. 4, No. 3, 2009, pp. 147-156.
- [29] M. Rezaei, M. Khajenoori and B. Nematollahi, "Synthesis of High Surface Area Nanocrystalline MgO by Pluronic P123 Triblock Copolymer Surfactant," *Powder Technology*, Vol. 205, No. 1-3, 2011, pp. 112-116. <http://dx.doi.org/10.1016/j.powtec.2010.09.001>
- [30] C. Chizallet, G. Costentin, H. Lauron-Pernot, M. Che, C. Bonhomme, J. Maquet, F. Delbecq and P. Sautet, "Study of the Structure of OH Groups on MgO by 1d and 2d ¹H MAS NMR Combined with DFT Cluster Calculations," *The Journal of Physical Chemistry C*, Vol. 111, No. 49, 2007, pp. 18279-18287. <http://dx.doi.org/10.1021/jp077089g>
- [31] Y. V. Larichev, B. L. Moroz, V. I. Zaikovskii, S. M. Yunusov, E. S. Kalyuzhnaya, V. B. Shur and V. I. Bukhtiyarov, "XPS and TEM Studies on the Role of the Support and Alkali Promoter in Ru/MgO and Ru-Cs/MgO Catalysts for Ammonia Synthesis," *The Journal of Physical Chemistry C*, Vol. 111, No. 26, 2007, pp. 9427-9436. <http://dx.doi.org/10.1021/jp066970b>
- [32] M. B. Kasture, P. Patel, A. A. Prabhune, C. V. Ramana, A. A. Kulkarni and B. L. V. Prasad, "Synthesis of Silver Nanoparticles by Sophorolipids: Effect of Temperature and Sophorolipid Structure on the Size of Particles," *Journal of Chemical Sciences*, Vol. 120, No. 6, 2008, pp. 515-520. <http://dx.doi.org/10.1007/s12039-008-0080-6>
- [33] J. Lv, L. Qiu and B. Qu, "Controlled Growth of Three Morphological Structures of Magnesium Hydroxide Nanoparticles by Wet Precipitation Method," *Journal of Crystal Growth*, Vol. 267, No. 3-4, 2004, pp. 676-684. <http://dx.doi.org/10.1016/j.jcrysgro.2004.04.034>
- [34] K. Mageshwari and R. Sathyamoorthy, "Studies on Photocatalytic Performance of MgO Nanoparticles Prepared by Wet Chemical Method," *Transactions of the Indian Institute of Metals*, Vol. 65, No. 1, 2012, pp. 49-55. <http://dx.doi.org/10.1007/s12666-011-0106-5>
- [35] M. A. Boudreau, J. F. Fisher and S. Mobashery, "Messenger Functions of the Bacterial Cell Wall-Derived Muropeptides," *Biochemistry*, Vol. 51, No. 14, 2012, pp. 2974-2990. <http://dx.doi.org/10.1021/bi300174x>
- [36] A. Panacek, L. Kvitek, R. Prucek, M. Kolar, R. Vecerova, N. Pizurova, V. K. Sharma, T. J. Nevecna and R. Zboril, "Silver Colloid Nanoparticles: Synthesis, Characterization, and Their Antibacterial Activity," *The Journal of Physical Chemistry B*, Vol. 110, No. 33, 2006, pp. 16248-16253. <http://dx.doi.org/10.1021/jp063826h>
- [37] X. Pan, Y. Wang, Z. Chen, D. Pan, Y. Cheng, Z. Liu, Z. Lin and X. Guan, "Investigation of Antibacterial Activity and Related Mechanism of a Series of Nano-Mg(OH)₂," *ACS Applied Materials & Interfaces*, Vol. 5, No. 3, 2013, pp. 1137-1142. <http://dx.doi.org/10.1021/am302910q>
- [38] K. Rishnamoorthy, J. Y. Moon, H. B. Hyun, S. K. Cho and S.-J. Kim, "Mechanistic Investigation on the Toxicity of MgO Nanoparticles toward Cancer Cells," *Journal of Materials Chemistry*, Vol. 22, No. 47, 2012, pp. 24610-24617. <http://dx.doi.org/10.1039/c2jm35087d>